



Light WIMPs, Equivalent Neutrinos, BBN, And The CMB

Gary Steigman^{1,2,3} and Kenneth M. Nollett^{2,4}

¹ Physics Department, The Ohio State University, Columbus, Ohio, USA

² Center for Cosmology and Astro-Particle Physics, The Ohio State University, Columbus, Ohio, USA

³ Departamento de Astronomia, Universidade de São Paulo, São Paulo, Brasil
e-mail: steigman.1@osu.edu

⁴ Department of Physics and Astronomy, Ohio University, Athens, Ohio, USA
e-mail: nollett@ohio.edu

Abstract. Recent updates to the observational determinations of the primordial abundances of helium (^4He) and deuterium are compared to the predictions of BBN to infer the universal ratio of baryons to photons, $\eta_{10} \equiv 10^{10}(n_{\text{B}}/n_{\gamma})_0$ (or, the present Universe baryon mass density parameter, $\Omega_{\text{B}}h^2 = \eta_{10}/273.9$) as well as to constrain the effective number of neutrinos (N_{eff}) and the number of equivalent neutrinos (ΔN_{ν}). These BBN results are compared to those derived independently from the Planck CMB data. In the absence of a light WIMP ($m_{\chi} \gtrsim 20$ MeV), $N_{\text{eff}} = 3.05(1 + \Delta N_{\nu}/3)$. In this case, there is excellent agreement between BBN and the CMB but, the joint fit reveals that $\Delta N_{\nu} = 0.40 \pm 0.17$, disfavoring standard big bang nucleosynthesis (SBBN) ($\Delta N_{\nu} = 0$) at $\sim 2.4\sigma$, as well as a sterile neutrino ($\Delta N_{\nu} = 1$) at $\sim 3.5\sigma$. In the presence of a light WIMP ($m_{\chi} \lesssim 20$ MeV), the relation between N_{eff} and ΔN_{ν} depends on the WIMP mass, leading to degeneracies among N_{eff} , ΔN_{ν} , and m_{χ} . The complementary and independent BBN and CMB data can break some of these degeneracies. Depending on the nature of the light WIMP (Majorana or Dirac fermion, real or complex scalar) the joint BBN + CMB analyses set a **lower** bound to m_{χ} in the range 0.5 – 5 MeV ($m_{\chi}/m_e \gtrsim 1 - 10$) and, they identify **best fit** values for m_{χ} in the range 5 – 10 MeV. The joint BBN + CMB analyses find a **best fit** value for the number of equivalent neutrinos, $\Delta N_{\nu} \approx 0.65$, nearly independent of the nature of the WIMP. The best fit still disfavors the absence of dark radiation ($\Delta N_{\nu} = 0$ at $\sim 95\%$ confidence), while allowing for the presence of a sterile neutrino ($\Delta N_{\nu} = 1$ at $\lesssim 1\sigma$). For all cases considered here, the lithium problem persists. These results, presented at the Rencontres de l'Observatoire de Paris 2013 - ESO Workshop and summarized in these proceedings, are based on Nollett & Steigman (2013).

Key words. Cosmology: primordial nucleosynthesis – Cosmology: early Universe – Cosmology: cosmological parameters – Cosmology: cosmic background radiation

1. Introduction

Late in the early evolution of the Universe, after the e^{\pm} pairs have annihilated, the only re-

Send offprint requests to: G. Steigman

maining standard model (SM) particles are the CMB photons and the three relic neutrinos (ν_e, ν_μ, ν_τ). At these early epochs the Universe is “radiation dominated”, and after the e^\pm pairs have annihilated, the energy density may be written as $\rho_R = \rho_\gamma + 3\rho_\nu$, where $3\rho_\nu$ accounts for the contributions from the three, SM neutrinos. In addition to the SM neutrinos, there may be additional, beyond the standard model particles that, like the SM neutrinos, are extremely light ($\lesssim 10$ eV) and very weakly interacting. During the early (or, even, relatively late) evolution of the Universe these “extra”, neutrino-like particles, so called “equivalent neutrinos”, will contribute to the energy density, which controls the early Universe expansion rate. If ΔN_ν counts the contribution of equivalent neutrinos, often referred to as “dark radiation”, $\rho_R = \rho_\gamma + (3 + \Delta N_\nu)\rho_\nu$. The contribution to ΔN_ν of an equivalent neutrino that decouples along with the SM neutrinos (at $T = T_{\nu d}$) will be $\Delta N_\nu = 1$ for a Majorana fermion (*e.g.*, a sterile neutrino), $\Delta N_\nu = 2$ for a Dirac fermion or, $\Delta N_\nu = 4/7$ for a real scalar. In general, ΔN_ν is an integer (fermions) or an integer multiple of $4/7$ (bosons). However, an equivalent neutrino that is more weakly interacting than the SM neutrinos, will have decoupled earlier in the evolution of the Universe and its contribution to ΔN_ν will be suppressed by the heating of the SM neutrinos (and photons) when the heavier SM particles decay and/or annihilate. Therefore, in principle, there is no reason that ΔN_ν should be an integer or an integer multiple of $4/7$ (for further discussion see Steigman (2013); for a specific example of three, very weakly coupled, right-handed neutrinos, see Anchordoqui et al. (2013)).

After the SM neutrinos have decoupled, when $T = T_{\nu d} \approx 2 - 3$ MeV, the e^\pm pairs annihilate, heating the photons but not the already decoupled neutrinos. Prior to neutrino decoupling (and e^\pm annihilation), the neutrinos, e^\pm pairs, and the photons are in equilibrium at the same temperature, $T_\nu = T_e = T_\gamma$ but, after e^\pm annihilation, the photons are hotter than the relic neutrinos. In the simplest, textbook discussions, it is assumed that the neutrinos decoupled instantaneously and that the electrons were effectively mass-

less at neutrino decoupling, when $T_e = T_{\nu d}$. With these approximations, the late time (after e^\pm annihilation is complete) ratio of neutrino and photon temperatures is $(T_\nu/T_\gamma)_0 = (4/11)^{1/3}$ and the ratio of energy densities in one species of neutrino (ρ_ν^0) and the photons is $(\rho_\nu^0/\rho_\gamma)_0 = 7/8(T_\nu/T_\gamma)_0^4 = 7/8(4/11)^{4/3}$. However, at neutrino decoupling $m_e/T_{\nu d} \approx 0.2 \neq 0$ and, ρ_ν differs (by a small amount) from ρ_ν^0 (Steigman 2013). Furthermore, the neutrinos don’t decouple instantaneously and, while the neutrinos are partially coupled they share some (a small amount) of the energy released by e^\pm annihilation (Mangano et al. 2005). These effects can be accounted for by introducing N_{eff} , the “effective number of neutrinos”, where $\rho_R \equiv \rho_\gamma + N_{\text{eff}}\rho_\nu^0$, so that,

$$N_{\text{eff}} = 3 \left[\frac{11}{4} \left(\frac{T_\nu}{T_\gamma} \right)_0 \right]^{4/3} \left(1 + \frac{\Delta N_\nu}{3} \right). \quad (1)$$

Assuming instantaneous neutrino decoupling and that $m_e \ll T_{\nu d}$, $N_{\text{eff}} = 3 + \Delta N_\nu$. Assuming instantaneous decoupling but correcting for the finite electron mass, $N_{\text{eff}} \approx 3.02(1 + \Delta N_\nu/3)$ (Steigman 2013). Accounting for non-instantaneous neutrino decoupling and for the finite electron mass, $N_{\text{eff}} \approx 3.05(1 + \Delta N_\nu/3)$ (Mangano et al. 2005). In addition, in this case there is a very small, but not entirely negligible correction to the BBN predicted primordial helium abundance (Mangano et al. 2005).

So far, the possibility of a very light, weakly interacting, massive particle, a WIMP χ , has been ignored. The difference between a WIMP and an equivalent neutrino is that a WIMP remains thermally coupled to the SM particles after it has become non-relativistic and when it begins annihilating and, its annihilation heats the remaining SM particles (either the photons and, possibly, the e^\pm pairs if the WIMP couples electromagnetically or, the SM neutrinos if the WIMP only couples to them). Note that in the analysis and discussion here, the WIMP **need not** be the dark matter; it could be a sub-dominant component of the dark matter ($\Omega_\chi < \Omega_{\text{CDM}}$). Here we specialize to the case of a light WIMP coupled only to the photons and e^\pm pairs. The relevant role played by such a light WIMP is that its annihilation heats

the photons relative to the decoupled SM neutrinos, changing (reducing) $(T_\nu/T_\gamma)_0$. In this case, N_{eff} is a function of m_χ (see Steigman (2013) and references therein). The expansion rate of the early Universe, the Hubble parameter H , is controlled by the energy density ($H \propto \rho_R^{1/2}$), so any modification of N_{eff} will be reflected in a non-standard expansion rate (e.g., during BBN). Extremely light WIMPs ($m_\chi \lesssim m_e$) will annihilate so late that, if their annihilation produces photons, they will modify the baryon-to-photon ratio ($\eta_{10} = 10^{10}(n_B/n_\gamma)_0 = 273.9\Omega_B h^2$) during or after BBN. BBN can probe N_{eff} as well as the universal ratio of baryons-to-photons. At late times, e.g., at recombination, the CMB can also probe $\Omega_B h^2$ and N_{eff} . As independent probes of the effective number of neutrinos (N_{eff}) or the number of equivalent neutrinos (ΔN_ν) and the universal baryon density ($\Omega_B h^2$ or η_{10}), BBN and the CMB can help to break the degeneracies among these parameters and the WIMP mass (and spin/statistics) and to constrain their allowed ranges (see, Steigman (2013) and Fig. 1).

1.1. Planck CMB Constraints

In the analysis in Nollett & Steigman (2013), whose results are described and summarized here, the CMB constraints on $\Omega_B h^2$ and N_{eff} are adopted from the Planck $\Lambda\text{CDM} + N_{\text{eff}}$ fit including BAO (Planck Collaboration 2013). The correlations between these quantities have been included in our analysis. For our analysis we have adopted $\Omega_B h^2 = 0.0223 \pm 0.0003$ ($\eta_{10} = 6.11 \pm 0.08$) and $N_{\text{eff}} = 3.30 \pm 0.27$. In Fig. 1, the Planck 68% and 95% constraints on N_{eff} are shown as a function of the WIMP mass (the CMB constraints are independent of the WIMP mass). Also shown are the curves corresponding to N_{eff} as a function of m_χ for a Majorana fermion WIMP and for three choices of the number of equivalent neutrinos. The behavior seen here is qualitatively similar for a Dirac or scalar WIMP (see, e.g., (Steigman 2013)). This figure illustrates the degeneracies between N_{eff} and m_χ . For example, for $\Delta N_\nu = 0$ the CMB can set a **lower** bound to m_χ . In

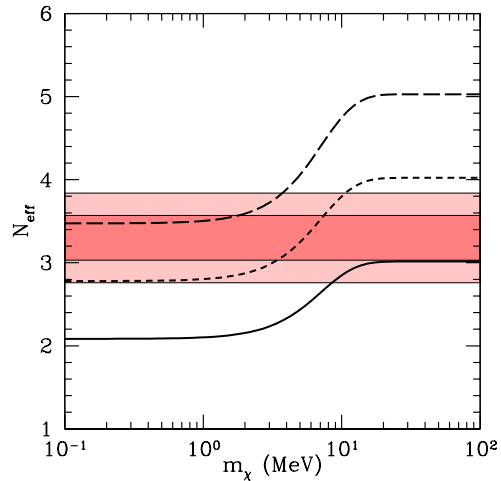


Fig. 1. N_{eff} is shown as a function of the WIMP mass for ΔN_ν equivalent neutrinos, for the case of a Majorana fermion WIMP. The solid curve is for $\Delta N_\nu = 0$, the short dashed curve is for $\Delta N_\nu = 1$, and the long dashed curve is for $\Delta N_\nu = 2$. The horizontal, red bands are the Planck CMB 68% and 95% allowed ranges. This figure is from Nollett & Steigman (2013); an earlier version is in Steigman (2013).

contrast, for $\Delta N_\nu = 1$ (2), high values of m_χ are excluded.

1.2. BBN Constraints

Of the light nuclides produced during BBN, D and ^4He are the relic nuclei of choice. To account for, or minimize, the post-BBN contributions to the primordial abundances, observations at high redshift (z) and/or low metallicity (Z) are preferred. Deuterium (and hydrogen) is observed in high- z , low- Z , QSO absorption line systems and helium is observed in relatively low- Z , extragalactic H II regions. Even so, it may still be necessary to correct for any post-BBN nucleosynthesis that may have modified their primordial abundances. The post-BBN evolution of D and ^4He is simple and monotonic. As gas is cycled through stars, D is destroyed and ^4He produced. Finally, D and ^4He provide complementary probes of the parameters of interest. $y_{\text{DP}} \equiv 10^5(\text{D}/\text{H})_{\text{P}}$ is

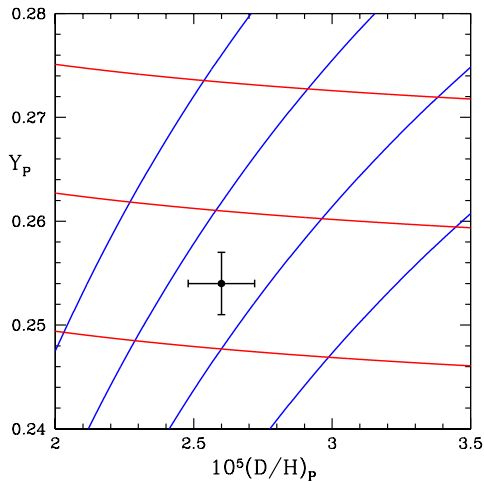


Fig. 2. BBN predicted curves of constant baryon-to-photon ratio and equivalent number of neutrinos in the $Y_P - y_{DP}$ plane. From left to right (blue), $\eta_{10} = 7.0, 6.5, 6.0, 5.5$. From bottom to top (red) $\Delta N_\nu = 0, 1, 2$. Also shown by the filled circle and error bars are the observationally inferred values of Y_P and y_{DP} adopted here (see the text).

mainly sensitive to the baryon density at BBN ($\Omega_B h^2$) and is less sensitive to ΔN_ν . In contrast, the ${}^4\text{He}$ mass fraction, Y_P , is very insensitive to $\Omega_B h^2$, but is quite sensitive to ΔN_ν . This complementary, nearly orthogonal, dependence of D and Y_P on η_{10} and ΔN_ν is illustrated in Fig. 2. For the analysis here (and in Nollett & Steigman (2013)), we have adopted, $y_{DP} = 2.60 \pm 0.12$ (Pettini & Cooke 2012) and $Y_P = 0.254 \pm 0.003$ (Izotov et al. 2013).

In contrast, ${}^3\text{He}$ has a more complicated, model dependent, post-BBN evolution and has only been observed in the relatively metal-rich interstellar medium of the Galaxy. In addition, its BBN-predicted abundance is less sensitive to $\Omega_B h^2$ and ΔN_ν than that of D . ${}^3\text{He}$ is not used in our BBN analysis but, we have confirmed that its observationally inferred primordial abundance (Bania et al. 2002) is in good agreement with our BBN-predicted results. ${}^7\text{Li}$ suffers from some of the same issues as ${}^3\text{He}$. Its post-BBN evolution is complicated and model dependent. Although, in principle, ${}^7\text{Li}$ could be as useful as D in constraining $\Omega_B h^2$ (and, to

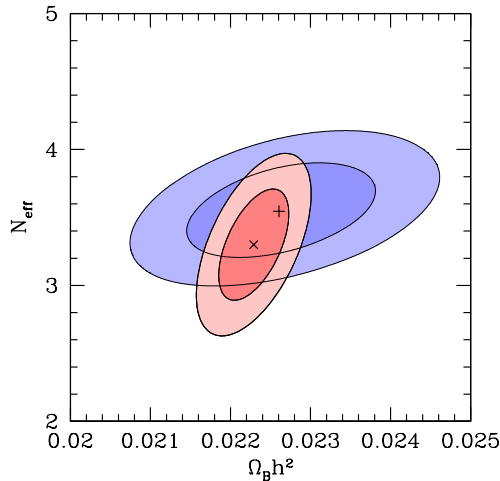


Fig. 3. A comparison of the the 68% (darker) and 95% (lighter) contours in the $N_{\text{eff}} - \Omega_B h^2$ plane derived separately from BBN (blue) and the CMB (pink). The “x” symbol marks the best fit CMB point and the “+” is the best fit BBN point.

a lesser extent, ΔN_ν), there is the well known “lithium problem” (see, *e.g.*, Fields (2011) and Spite et al. (2012) for recent reviews) that, as will be seen below, persists. In the BBN analyses, with and without a light WIMP, only D and ${}^4\text{He}$ are used to constrain $\Omega_B h^2$ and ΔN_ν (or, N_{eff}) and these BBN constraints are compared to the independent constraints from the CMB.

2. BBN Without A Light WIMP

In the absence of a light WIMP the BBN-predicted primordial abundances depend on only two parameters, the baryon-to-photon ratio (η_{10} or, $\Omega_B h^2$) and the number of equivalent neutrinos (ΔN_ν). In the absence of a light WIMP the effective number of neutrinos and the number of equivalent neutrinos are related by $N_{\text{eff}} = 3.05(1 + \Delta N_\nu/3)$. With two, independent relic abundances (D and ${}^4\text{He}$), BBN can constrain these two parameters. This is illustrated in Fig. 2. For the abundances adopted here, we find from BBN (without a light WIMP), $\eta_{10} = 6.19 \pm 0.21$ ($\Omega_B h^2 = 0.0226 \pm 0.0008$) and $\Delta N_\nu = 0.51 \pm 0.23$, corresponding to $N_{\text{eff}} = 3.56 \pm 0.23$ (accounting for

round-off). The BBN 68% and 95% contours in the $N_{\text{eff}} - \Omega_B h^2$ plane, along with the best fit point, are shown in Fig. 3, where they are compared to the corresponding contours (and best fit point) for these parameters inferred from the Planck CMB data (Planck Collaboration 2013). As Fig. 3 reveals, in the absence of a light WIMP, there is excellent agreement between BBN and the CMB. This motivates (justifies) a joint BBN + CMB analysis, resulting in (for the joint fit) $\eta_{10} = 6.13 \pm 0.07$ ($\Omega_B h^2 = 0.0224 \pm 0.0003$) and $N_{\text{eff}} = 3.46 \pm 0.17$ ($\Delta N_\nu = 0.40 \pm 0.17$). However, as may be seen from Fig. 4, this joint BBN + CMB fit favors neither standard BBN (SBBN: $\Delta N_\nu = 0$), nor the presence of a sterile neutrino ($\Delta N_\nu = 1$). SBBN is disfavored at $\sim 2.4 \sigma$ and a sterile neutrino is disfavored at $\sim 3.5 \sigma$.

As for lithium, for the joint BBN + CMB parameter values the BBN predicted ${}^7\text{Li}$ abundance is $A(\text{Li}) \equiv 12 + \log(\text{Li}/\text{H}) = 2.72 \pm 0.04$, to be compared with the observationally inferred ‘‘Spite Plateau’’ abundance of $A(\text{Li}) = 2.20 \pm 0.06$ (Spite et al. 2012). The lithium problem, the factor of ~ 3 difference between predictions and observations, persists.

3. BBN With A Light WIMP

Although BBN and the CMB are in excellent agreement in the absence of a light WIMP, we are interested in investigating the constraints they can set on the mass of such a WIMP and also, how its presence changes the parameter constraints discussed in the previous section. The presence of a light WIMP can effect BBN (and the CMB) in several ways, provided it is sufficiently light. For example, a very light WIMP might be mildly relativistic at BBN (or, prior to BBN, when the neutron-to-proton ratio is being set), contributing to the total energy density (similar to an equivalent neutrino) and speeding up the expansion rate. A faster expansion generally increases the neutron-to-proton ratio at BBN, leading to the production of more ${}^4\text{He}$. Also, such a very light WIMP might annihilate during or after BBN and the photons produced by its annihilation will change the baryon-to-photon ratio from its value during BBN. The baryon-to-photon ratio at present

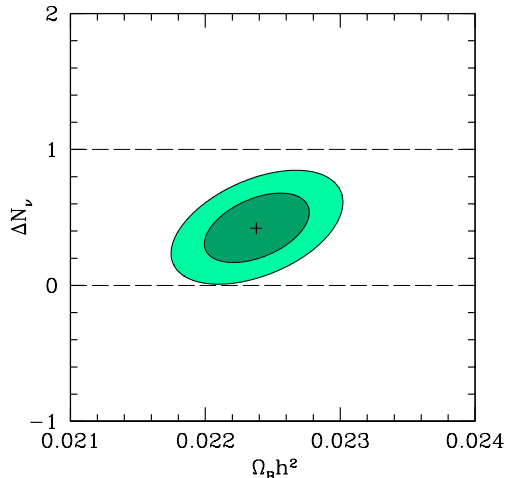


Fig. 4. The joint BBN+CMB 68% (darker) and 95% (lighter) contours in the number of equivalent neutrinos (ΔN_ν) – baryon density ($\Omega_B h^2$) plane. The ‘‘+’’ symbol marks the best fit point. SBBN corresponds to $\Delta N_\nu = 0$ and a sterile neutrino corresponds to $\Delta N_\nu = 1$, as shown by the dashed lines.

may differ from its value at BBN affecting, mainly, the BBN D abundance. The effects on the BBN light element yields in the presence of a light WIMP but, neglecting any equivalent neutrinos ($\Delta N_\nu \equiv 0$), were investigated by Kolb et al. (1986) and Serpico & Raffelt (2004) and, more recently, by Boehm et al. (2013). In Nollett & Steigman (2013) those BBN calculations were extended to allow for the presence of dark radiation ($\Delta N_\nu \neq 0$). In this case, there are three free parameters. In addition to the baryon density (η_{10} or $\Omega_B h^2$) and the number of equivalent neutrinos (ΔN_ν), the light WIMP mass is allowed to vary, modifying the connection between N_{eff} and ΔN_ν ,

$$N_{\text{eff}} = N_{\text{eff}}^0(m_\chi)(1 + \Delta N_\nu/3), \quad (2)$$

and producing time-dependent effects on the weak rates and the expansion rate during BBN. As already noted by Kolb et al. (1986), Serpico & Raffelt (2004) and, Boehm et al. (2013), for an electromagnetically coupled light WIMP, as m_χ decreases below ~ 20 MeV, the BBN predicted D abundance decreases monotonically, while the ${}^4\text{He}$ abundance first decreases (very

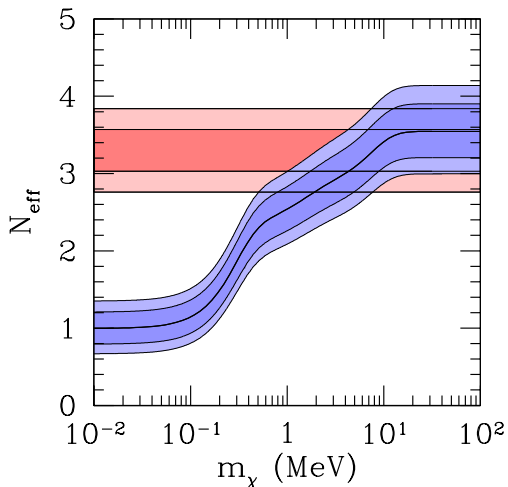


Fig. 5. The CMB and BBN constraints on N_{eff} as a function of the light WIMP mass, m_χ . The horizontal, pink bands show the 68% and 95% ranges from the Planck CMB results. The blue bands show the corresponding BBN ranges. The black curve through the middle of the blue bands shows the values of N_{eff} as a function of m_χ for which the BBN predicted D and ${}^4\text{He}$ abundances agree exactly with the observationally inferred abundances adopted here.

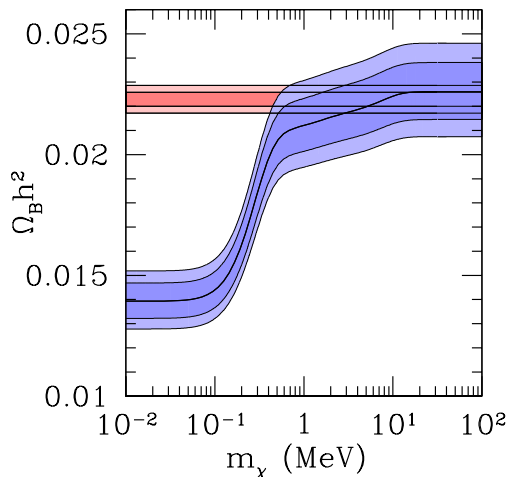


Fig. 6. As in Fig. 5, the CMB and BBN constraints on $\Omega_{\text{B}}h^2$ as a function of the light WIMP mass, m_χ .

slightly) and then increases monotonically. For a more detailed discussion of the physics controlling this modified BBN, especially the non-monotonic behavior of Y_{p} and its connection to the temperature dependence of the neutron – proton interconversion reactions, see Nollett & Steigman (2013).

With three parameters and two observables (Y_{DP} and Y_{p}), BBN is underconstrained. For each choice of m_χ , a pair of η_{10} and ΔN_ν parameters can be found so that BBN predicts – exactly – the observed D and ${}^4\text{He}$ abundances. This is illustrated in Figs. 5 and 6, which show N_{eff} and $\Omega_{\text{B}}h^2$ as functions of the WIMP mass, as inferred from the CMB (N_{eff} and $\Omega_{\text{B}}h^2$ are independent of m_χ) and from BBN. These figures show how the degeneracy illustrated in Fig. 1 can be broken by combining constraints from the CMB with those from BBN.

A comparison of the BBN and CMB constraints on N_{eff} and $\Omega_{\text{B}}h^2$ is shown in Fig. 7. The independent and complementary BBN and

CMB results are in excellent agreement, over the range in N_{eff} and $\Omega_{\text{B}}h^2$ defined by the Planck CMB constraints. As a result, the BBN and CMB results may be combined in a joint analysis to identify the allowed 68% and 95% ranges in the N_{eff} (or, ΔN_ν) – $\Omega_{\text{B}}h^2$ plane. This joint analysis (Nollett & Steigman 2013) finds $N_{\text{eff}} = 3.30 \pm 0.26$ and $\Omega_{\text{B}}h^2 = 0.0223 \pm 0.0003$ ($\eta_{10} = 6.11 \pm 0.08$), consistent with the CMB results alone, but with slightly smaller uncertainties. The new results from this joint analysis for ΔN_ν as a function of $\Omega_{\text{B}}h^2$ are shown in Fig. 8. For the joint fit, $\Delta N_\nu = 0.65^{+0.46}_{-0.35}$. Note that these figures and the numerical results cited here are for the case of a Majorana fermion WIMP. Very similar results are found for a Dirac fermion or for a real or complex scalar WIMP (see Table 1 in Nollett & Steigman (2013)).

Allowing for a light WIMP, the joint CMB + BBN comparison excludes light WIMPs with masses $\lesssim 0.5 - 5$ MeV. The best joint fit WIMP mass is found to be $m_\chi \approx 5 - 10$ MeV, depending on the nature of the WIMP. However, very nearly independently of the nature of the WIMP, the best fit for the dark radiation is $\Delta N_\nu \approx 0.65$ in all cases (see Fig. 10 and Table 1 in Nollett & Steigman (2013)). While $\Delta N_\nu = 0$ is still disfavored at $\sim 95\%$ confidence, in the presence of light WIMP, a ster-

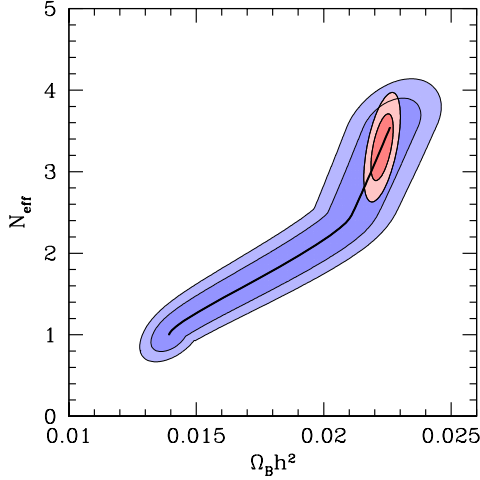


Fig. 7. The CMB and BBN constraints on N_{eff} as a function of the baryon density $\Omega_{\text{B}}h^2$ (combining the results shown in Figs. 5 & 6).

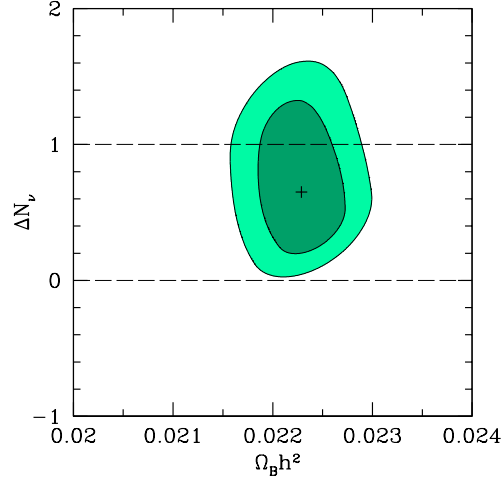


Fig. 8. The joint CMB + BBN constraints on dark radiation (ΔN_{ν}) as a function of the baryon density ($\Omega_{\text{B}}h^2$). The dashed lines indicate the absence of dark radiation ($\Delta N_{\nu} = 0$) and the presence of a sterile neutrino ($\Delta N_{\nu} = 1$).

ile neutrino (but, not two sterile neutrinos!) is now permitted. Since the no light WIMP case is a good fit to the BBN and CMB data, there is no upper bound to the WIMP mass.

It is interesting that for the WIMP masses allowed by the joint BBN + CMB fit (including the high WIMP mass limit – the no light WIMP case), the BBN predicted lithium abundance lies in the range $A(\text{Li}) = 2.72 \pm 0.04$ (see Fig. 13 in Nollett & Steigman (2013)), still a factor of ~ 3 larger than the observationally inferred Spite Plateau value of $A(\text{Li}) = 2.20 \pm 0.06$ (Spite et al. 2012). A light WIMP does not help to alleviate (indeed, it reinforces) the lithium problem.

4. Summary And Conclusions

In the absence of a light WIMP the effective number of neutrinos and the number of equivalent neutrinos are simply related, $N_{\text{eff}} = 3.05(1 + \Delta N_{\nu}/3)$ and the Planck CMB data alone, $N_{\text{eff}} = 3.30 \pm 0.27$ (Planck Collaboration 2013), constrains $\Delta N_{\nu} = 0.25 \pm 0.27$, consistent with the absence of dark radiation at $\lesssim 1\sigma$ (and, inconsistent with a sterile neutrino at $\sim 2.8\sigma$). The CMB alone also provides a constraint on the universal baryon density,

$\Omega_{\text{B}}h^2 = 0.0223 \pm 0.0003$ ($\eta_{10} = 6.11 \pm 0.08$). For $\Delta N_{\nu} = 0$ and the Planck value of the baryon density, BBN (SBBN) predicts the primordial D abundance to be $y_{\text{DP}} = 2.48 \pm 0.05$, in excellent agreement with the observationally inferred value of $y_{\text{DP}} = 2.60 \pm 0.12$ (Pettini & Cooke 2012). However, for this combination of $\Omega_{\text{B}}h^2$ and ΔN_{ν} , the SBBN predicted primordial helium abundance is $Y_{\text{p}} = 0.2472 \pm 0.0005$, which is $\sim 2.3\sigma$ away from the observationally inferred value, $Y_{\text{p}} = 0.254 \pm 0.003$ (Izotov et al. 2013). Independent of the CMB, in the absence of a light WIMP BBN provides independent constraints on ΔN_{ν} (N_{eff}) and $\Omega_{\text{B}}h^2$. BBN alone finds $\Delta N_{\nu} = 0.51 \pm 0.23$ ($N_{\text{eff}} = 3.56 \pm 0.23$) and $\Omega_{\text{B}}h^2 = 0.0226 \pm 0.0008$ ($\eta_{10} = 6.19 \pm 0.21$). Within the errors, the BBN and CMB constraints on N_{eff} and $\Omega_{\text{B}}h^2$ (ΔN_{ν} and η_{10}) are in excellent agreement. However, neither SBBN ($\Delta N_{\nu} = 0$) nor a sterile neutrino ($\Delta N_{\nu} = 1$) is favored by the combined BBN + CMB analysis, which finds $\Delta N_{\nu} = 0.40 \pm 0.17$. Indeed, in the absence of a light WIMP, $\Delta N_{\nu} = 0$ is disfavored at $\sim 2.4\sigma$ and $\Delta N_{\nu} = 1$ is disfavored at $\sim 3.5\sigma$. The joint BBN + CMB analysis predicts a primordial lithium abundance

$A(\text{Li}) = 2.72 \pm 0.04$, a factor of ~ 3 higher than the observationally inferred, primordial value; the “lithium problem” persists.

In the presence of a sufficiently light WIMP ($m_\chi \lesssim 20 \text{ MeV}$) the CMB results are unchanged (although the connection between N_{eff} and ΔN_ν is modified depending on the WIMP mass). In this case $N_{\text{eff}} = N_{\text{eff}}^0(m_\chi)(1 + \Delta N_\nu/3)$ and there is a degeneracy between the CMB constraints on N_{eff} and ΔN_ν (and m_χ). As may be seen from Fig. 1, for some choices of ΔN_ν , the CMB constraint on N_{eff} sets a lower limit to m_χ , while for other choices the CMB sets an upper limit to the WIMP mass. The independent constraints from BBN can help to break these degeneracies. In the presence of a light WIMP BBN depends on three parameters: ΔN_ν , N_{eff} , $\Omega_B h^2$ (or, m_χ , ΔN_ν , η_{10}) but, there are only two BBN constraints from D and ${}^4\text{He}$. For each choice of m_χ , there is always a pair of ΔN_ν and η_{10} values for which BBN predicts – exactly – the observationally inferred primordial D and ${}^4\text{He}$ abundances. However, the corresponding BBN inferred values (and ranges) of N_{eff} and $\Omega_B h^2$ need not agree with the values (and ranges) set by the CMB. By comparing the BBN and CMB constraints, the degeneracies may be broken. In this way a lower bound, as well as a best fit value, of the WIMP mass is found (depending on the nature of the WIMP). For the case of a Majorana fermion WIMP shown in the figures, $m_\chi \gtrsim 1.7 \text{ MeV}$ and the best fit is for a WIMP mass $m_\chi = 7.9 \text{ MeV}$. Depending on the nature of the WIMP, the lower bound to m_χ ranges from $\sim m_e$ to $\sim 10 m_e$, while the best fit WIMP masses lie in the range $\sim 5 - 10 \text{ MeV}$ (see Nollett & Steigman (2013)). In all cases, very nearly independent of the nature of the WIMP, $\Delta N_\nu \approx 0.65$. While the joint BBN + CMB analysis finds essentially the CMB values for N_{eff} and $\Omega_B h^2$, the presence of an additional, free parameter relaxes the constraints (increases the error) on ΔN_ν (compared to the no light WIMP case). Now, a sterile neutrino is permitted at $\lesssim 68\%$ confidence (see Fig. 8). However, the absence of dark radiation ($\Delta N_\nu = 0$) is still disfavored at $\sim 95\%$ confidence. For the joint BBN + CMB analysis the BBN predicted primordial lithium abundance is $A(\text{Li}) =$

2.73 ± 0.04 , a factor of ~ 3 higher than the observationally inferred value. Even in the presence of a light WIMP, the lithium problem persists.

It should be noted that at this meeting R. Cooke presented new results on the primordial abundance of deuterium, $y_{\text{DP}} = 2.53 \pm 0.04$ (Cooke et al. 2013). Although the new central value agrees very well with the earlier, Pettini & Cooke (2012) result adopted here, the new uncertainty is smaller by a factor of three. In the analysis described here (and, in more detail in Nollett & Steigman (2013)), this small change in the primordial deuterium abundance has the effect of increasing η_{10} by ~ 0.1 and decreasing ΔN_ν by ~ 0.01 . These small changes, well within the errors, leave the results and conclusions presented here unaffected.

Acknowledgements. We are grateful to the Ohio State University Center for Cosmology and Astroparticle Physics for hosting K.M.N.’s visit during which most of the work described here was done. K.M.N is pleased to acknowledge support from the Institute for Nuclear and Particle Physics at Ohio University. G.S. is grateful for the hospitality provided by the Departamento de Astronomia of the Instituto Astronômico e Geofísico of the Universidade de São Paulo, where these proceedings were written. The research of G.S. is supported at OSU by the U.S. DOE grant DE-FG02-91ER40690.

References

- Anchordoqui, L., Goldberg, H., & Steigman, G. 2013, Phys. Lett. B, 718, 1162
- Bania, T. M., Rood, R. T., & Balser, D. S. 2002, Nature, 415, 54
- Boehm, C., Dolan, M. J., & McCabe, C. 2013, JCAP, 08, 041
- Cooke, R. J., Pettini, M., Jorgenson, R. A., Murphy, M. T., & Steidel, C. C. 2013, arXiv:1308.3240[astro-ph.CO]
- Fields, B. D. 2011, Ann. Rev. Nucl. Part. Sci., 61, 47
- Izotov, Y. I. Stasinska, G., & Guseva, N. G. 2013, A&A, 558, A57
- Kolb, E. W. Turner, M. S., & Walker, T. P. 1986, Phys. Rev. D, 34, 2197

- Mangano, G., Miele, G., Pastor, S., Pinto, T., Pisanti, O., & Serpico, P. D. 2005, Nucl. Phys. B, 729, 221
- Nollett, K. N. & Steigman, G. 2013, arXiv:1312.5725 [astro-ph.CO]
- Pettini, M. & Cooke R. 2012, MNRAS, 425, 2477
- Planck Collaboration, arXiv:1303.5076 [astro-ph.CO]
- Serpico, P. D. & Raffelt, G. G. 2004, Phys. Rev. D, 70, 043526
- Spite, M., Spite, F., & Bonifacio, P. 2012, Mem. Soc. Astron. Ital., 22, 9
- Steigman, G. 2013, Phys. Rev. D, 87, 103517